Mechanistical studies on the formation of carbon dioxide in extraterrestrial carbon monoxide ice analog samples

Chris J. Bennett, Corey S. Jamieson and Ralf I. Kaiser*

Received 20th January 2009, Accepted 11th March 2009
First published as an Advance Article on the web 1st April 2009
DOI: 10.1039/b901220f

Binary ice mixtures of two carbon monoxide isotopomers, $^{13}C^{16}O$ and $^{12}C^{18}O$, were subjected at 10 K to energetic electrons to investigate the interaction of ionizing radiation with extraterrestrial, carbon monoxide bearing ices. The chemical modifications were monitored on line and *in situ via* absorption–reflection–absorption Fourier transform infrared spectroscopy as well as in the gas-phase *via* a quadrupole mass spectrometer. Detected products include two newly formed carbon monoxide isotopomers ($^{12}C^{16}O$ and $^{13}C^{18}O$), carbon dioxide ($^{12}C^{16}O_2$, $^{12}C^{18}O^{16}O$, $^{12}C^{18}O_2$, $^{13}C^{16}O_2$, $^{13}C^{18}O^{16}O$, and $^{13}C^{18}O_2$), and dicarbon monoxide ($^{12}C^{13}C^{16}O$ and $^{13}C^{13}C^{16}O$). Kinetic profiles of carbon monoxide and of carbon dioxide were extracted and fit to derive reaction mechanisms and information on the decomposition of carbon monoxide and on the formation of carbon dioxide in extraterrestrial ice analog samples.

1. Introduction

In the gas-phase, carbon monoxide presents the second most prominent interstellar molecule with fractional abundances of typically 10^{-4}.[1] There are a number of routes to its formation in the gas-phase, which has been discussed elsewhere.[2] The depletion of gas-phase carbon monoxide is commonly associated with its adsorption onto interstellar grains during the collapse of a pre-stellar core.[3,4] Here, the abundance of carbon monoxide within interstellar ices from a recent survey of 23 infrared sources using the Infrared Space Observatory (ISO) found the abundance to vary between 3 to 25% relative to water.[5] Based on the fundamental band position and profile, the carbon monoxide molecule was found to reside in two distinct chemical environments: polar ices, which are dominated by water, and non-polar ices where carbon monoxide prevails; non-polar species like molecular nitrogen and molecular oxygen are thought to be also present in the non-polar ice component, although neither has been detected thus far, abundance limits of the latter with respect to CO have been deduced.[6] These grain particles are subjected to ionizing irradiation from ultraviolet (UV) photons as well as galactic cosmic ray (GCR) particles. This radiation field can chemically modify the pristine ices. UV photons typically have energies less than 13.6 eV[7] and only penetrate the outer monolayers of the ice-coated grains. Compositionally, GCRs consist of about 98% protons (p, H^+) and 2% helium nuclei (α-particles, He^{2+}).[8] Detailed collision cascade calculations demonstrate that energetic (>MeV) cosmic-ray particles can penetrate the entire icy grain.[9] It has been shown that in the case of a 10-MeV proton, 99.99% of the energy transferred into the ice target will be *via* an inelastic processes leading to ionization and/or vibrational excitation (followed by decomposition) of the target molecules; for a more detailed discussions on the effects of irradiation on ices, please refer to ref. 9–14.

The low abundance of carbon dioxide in the gas phase[15] but, on the other hand, the high abundances within interstellar ices of 8% to 35%, relative to water, leads to the postulation that carbon dioxide might be produced *via* radiolysis of carbon monoxide ices.[5] Indeed, the effects of ionizing radiation on pure carbon monoxide ices has been studied including the effects of UV radiation,[16–19] ion exposure,[17,19–23] and energetic electrons.[24] Among other species, such as linear carbon chains (C_3 and C_6), oxygen-terminated carbon clusters of the series C_nO (n = 2–7) and C_nO_2 (n = 3–5, 7), and carbon dioxide were observed, as postulated. However, despite the *qualitative* identification of carbon dioxide, the underlying formation routes and detailed mechanism have not been solved to date. Therefore, the focus of this paper is to arrive at an understanding of the mechanisms of the dissociation of carbon monoxide and the connected formation of carbon dioxide. Note that the formation of carbon dioxide has also been observed during the irradiation of differing ice mixtures,[25,26] and alternative proposed surface reactions exist;[27] the focal point here, however, is only to understand its formation within pure carbon monoxide ices. In order to facilitate mechanistical studies and to trace the carbon and oxygen atoms, we have isotopically labeled distinct atoms in carbon monoxide and studied binary ices of $^{13}C^{16}O$ and $^{12}C^{18}O$ at 10 K. For mechanistic studies, we focused on the interaction of these ices with energetic electrons, which are generated in the track of GCR particles penetrating ices, since these charged particles only divert energy to the molecules *via* inelastic interaction, but not in nuclear (elastic) energy transfer processes.

2. Experimental

The details of our experimental set-up, as well as the quantification of the column densities and ice thicknesses, can be found elsewhere.[24,28] Briefly, the experiments are conducted in an ultrahigh vacuum (UHV) chamber where

Department of Chemistry, University of Hawaii at Manoa, Honolulu, HI 96822, USA. E-mail: ralfk@hawaii.edu

oil-free magnetically suspended turbomolecular pumps are used to bring the base pressure down to around 5×10^{-11} torr. The gases are condensed onto a freely rotatable highly polished silver monocrystal situated in the center of the chamber which is cooled to 10 K by a closed cycle helium refrigerator. This condensed phase is sampled by a Nicolet 510 DX Fourier transform infrared (FTIR) spectrometer operating in absorption–reflection–absorption mode at a reflection angle of 75° (spectra are recorded in succession over the range 6000–400 cm^{-1} at a resolution of 2 cm^{-1}, each integrated over 2.5 min). Gaseous species are analyzed by a quadrupole mass spectrometer (Balzer QMG 420) operating in residual gas analyzer mode. During the actual experiment, a 1 : 1 mixture of $^{13}C^{16}O$: $^{12}C^{18}O$ gas mixture was initially prepared and condensed on the silver target for 7 min at a base pressure of 1×10^{-7} torr. Here, the overtone bands found at 4157 cm^{-1} and 4149 cm^{-1} were used to calculate the column densities of $^{13}C^{16}O$ and $^{12}C^{18}O$, respectively, where the absorption coefficient of 1.6×10^{-19} cm $molecule^{-1}$ is applied for both species.[29] Here, we derived a column density of $2.29 \pm 0.14 \times 10^{17}$ molecules cm^{-2} and $2.10 \pm 0.14 \times 10^{17}$ molecules cm^{-2}, respectively. Taking the molecular weights (29 $gmol^{-1}$ and 30 $gmol^{-1}$) and a density of 1.03 g cm^{-3},[30] we derive a thickness of 210 ± 10 nm. The ices were then irradiated with 5 keV electrons for 1 h at a beam current of 100 nA and scanned over a sample area of 1.8 ± 0.3 cm^2 with an electron gun (Specs EQ 22). However, the manufacturer states an electron extraction efficiency of 78.8%, reducing our *effective* current to 78.8 nA. The sample was then left isothermally at 10 K for 60 min to check the stability and reactivity of the species generated within the ice sample before the sample was heated to 300 K by a controlled heating program at a rate of 0.5 K min^{-1}.

3. Results

3.1 Infrared spectroscopy

3.1.1 Before irradiation. First, we present qualitative results of the irradiation induced chemistry (Fig. 1) and compare the infrared spectrum of the ice sample before (gray line) and after the radiation exposure (black line). The corresponding assignments are compiled in Table 1. The fundamental band positions of both isotopomers of carbon monoxide were found to absorb at 2090 cm^{-1} and 2086 cm^{-1} for ^{13}CO and $C^{18}O$, respectively. These features have been previously reported in solid carbon monoxide ices at 10 K with absorptions at 2092 and 2089 cm^{-1}, respectively.[31] Due to the purity of the isotopic labeling (99% ^{13}C for ^{13}CO and 95% ^{18}O for $C^{18}O$), we anticipate the presence of several other isotopomers of carbon monoxide. Indeed, the fundamental bands for CO were found at 2140 and 2136 cm^{-1} (corresponding to different matrix sites), compared to previously reported values of 2143 and 2139 cm^{-1}.[32] The $^{13}C^{18}O$ species was found to absorb at 2040 cm^{-1}; the same band position was reported in ref. 19. Due to the low natural abundance of the ^{17}O isotope of molecular oxygen (0.038%), the band occurring at 2111 cm^{-1} had previously been assigned to an interaction of carbon monoxide with the silver surface[24] in accordance with the experimental work of ref. 33, rather than from the $C^{17}O$ fundamental which also absorbs at this position (2112 cm^{-1}).[31] However, if this is the case, considering the relative concentrations of carbon monoxide isotopomers in our sample, we would expect to see additional, stronger peaks from the Ag–^{13}CO and Ag–$C^{18}O$ counterparts and possibly Ag–$^{13}C^{18}O$. Note that the $^{13}C^{17}O$ fundamental has recently been reported to absorb in this region, at 2065 cm^{-1}.[19] Although we find a carrier at 2064 cm^{-1}, it is around the same intensity as the band at 2111 cm^{-1}. For this reason, the bands at 2111 and 2064 cm^{-1} are assigned to $C^{17}O$ and $^{13}C^{17}O$. These features are shown in Fig. 1(b). The $2\nu_1$ overtone bands from carbon monoxide are also observable, with the CO molecule being found at 4254 cm^{-1} in accordance with previous studies.[31] For ^{13}CO and $C^{18}O$, the $2\nu_1$ overtone bands are shifted to 4157 and 4149 cm^{-1}, respectively (Fig. 1(c)).[30] The broad absorption peaking around 2158 cm^{-1} with a prominent shoulder at 2169 cm^{-1} is assigned to the combination band of the fundamental with the lattice modes.[31,34] The band at 2097 cm^{-1} can be assigned to the corresponding lattice mode for the $^{13}C^{18}O$ isotopomer.

It is important to note that all six anticipated isotopomers of the expected carbon dioxide product have all been identified to be present to a very small extent (less than 0.04% relative to carbon monoxide) within the initial ice mixture as minor side-products of the production process of the isotopically labeled carbon monoxide species. Here, the following isotopomers can be observed through the (ν_3) asymmetric stretch; CO_2 at 2346 cm^{-1}, ^{18}OCO at 2329 cm^{-1}, $C^{18}O_2$ at 2311 cm^{-1}, $^{13}CO_2$ at 2280 cm^{-1}, $^{18}O^{13}CO$ at 2263 cm^{-1}, and $^{13}C^{18}O_2$ at 2245 cm^{-1}.[35,36] Each of these features can be seen in Fig. 1(d). Lastly, the ν_2 degenerate bending mode can be found for $^{18}O^{13}CO$ (ν_2) was found at 636 cm^{-1}.

3.1.2 After irradiation. The effects of the irradiation are shown in Fig. 1 (black line); the corresponding peak assignments are compiled in Table 2. Based on the primary goal of our paper, this section will focus on the species relevant to the destruction of carbon monoxide and formation of distinct carbon dioxide isotopologues. Fig. 1(d) depicts the production of the isotopomers of carbon dioxide after the irradiation through the corresponding increased intensities of the ν_3 asymmetric stretching modes. It should be noted that for both the isotopomers $^{13}C^{18}O_2$ and CO_2, only a small amount is produced during the irradiation, whereby their presence in the original sample accounts for most of their abundance. On the other hand, it is evident that the other four isotopomers (^{18}OCO, $C^{18}O_2$, $^{13}CO_2$, and $^{18}O^{13}CO$) are produced in large quantities throughout the irradiation and in roughly equal proportions. Note that the increased abundance of these isotopomers of carbon dioxide allows additional bands to be observed in the infrared spectrum. Firstly, the $\nu_1 + \nu_3$ combination bands are found at 3714 and 3705 cm^{-1} for CO_2, 3668 and 3665 cm^{-1} for ^{18}OCO, and at 3626 cm^{-1} for $C^{18}O_2$ and $^{13}CO_2$.[35,37] The band at 3680 cm^{-1} can be tentatively assigned to the $\nu_1 + \nu_3$ combination band for ^{17}OCO. Secondly, the $2\nu_2 + \nu_3$ combination band was monitored for ^{18}OCO at 3561 cm^{-1}, for $C^{18}O_2$ and $^{13}CO_2$ at 3518 and 3515 cm^{-1}, and for $^{18}O^{13}CO$ at 3478 cm^{-1}.[35,37] Lastly, the ν_2

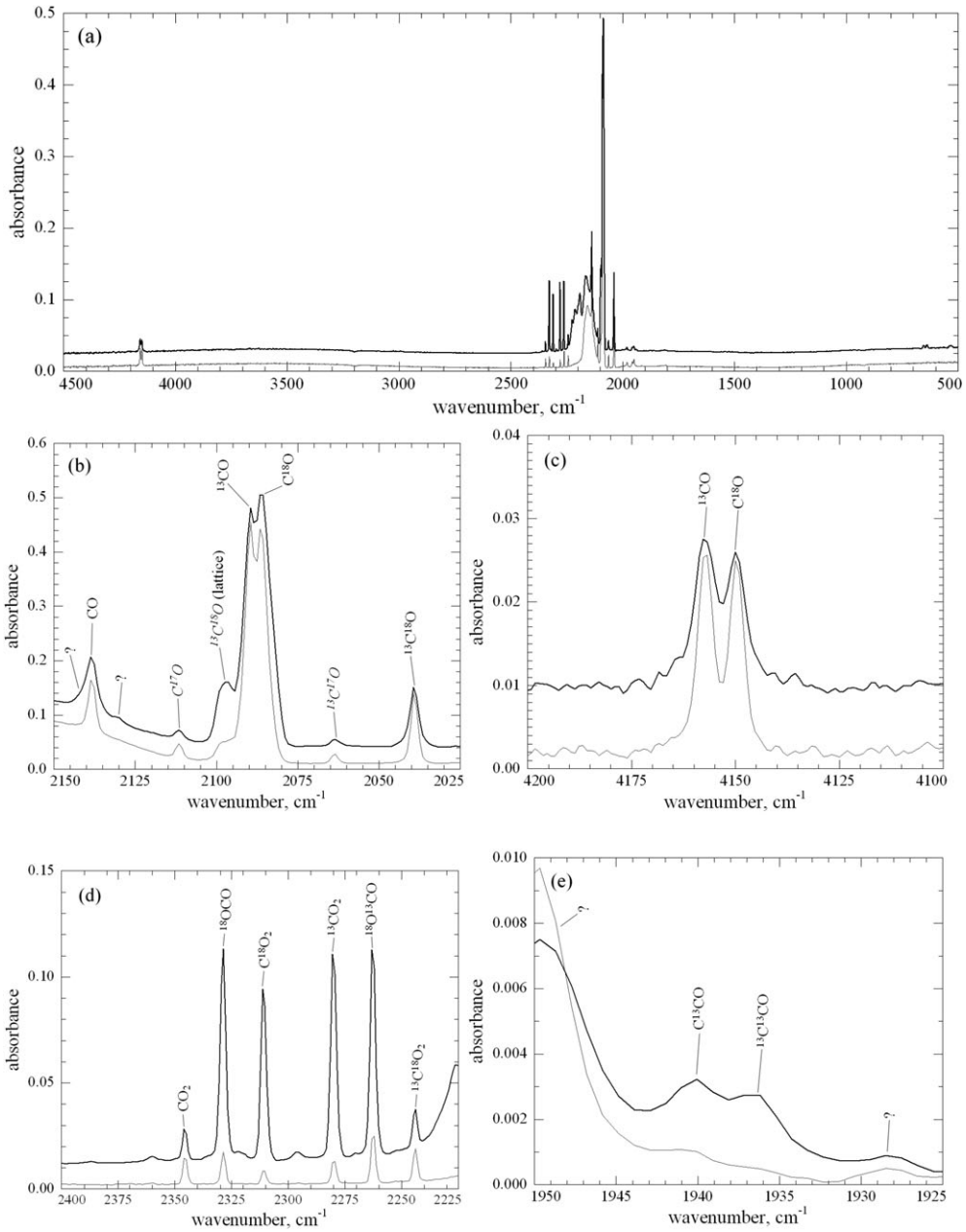

Fig. 1 Infrared spectrum of the $^{13}CO:C^{18}O$ ice mixture prior to (gray line) and after the irradiation (black line) shown over several different wavelength ranges: (a) 500–4500 cm^{-1}, (b) 2025–2150 cm^{-1}, (c) 4100–4200 cm^{-1}, (d) 2225–2400 cm^{-1}, and (e) 1925–1950 cm^{-1}. The absorption axis has been shifted for clarity. The unlabeled peaks in (d) at 2360, 2349, 2336, 2322, 2296 and 2271 cm^{-1} are attributed to the $\nu_2+\nu_4$ combination band of C_3O_2 isotopomers.

bending mode can be found at 654 cm^{-1} for ^{18}OCO, 650 cm^{-1} for $C^{18}O_2$, 640 cm^{-1} for $^{13}CO_2$ and at 636 cm^{-1} for $^{18}O^{13}CO$ (ν_2).

The dicarbon monoxide molecule (CCO) has previously been established as a product formed upon the irradiation of *pure* carbon monoxide ices.[24] However, the bands in the region around 1950 cm^{-1} prior to irradiation complicate the assignments for this species. It should be noted that the literature shows that the band position for the most intense band (ν_2; CO stretch) is highly dependant upon its chemical environment. Within argon matrices this vibration has been reported at 1969 cm^{-1},[38] yet in carbon monoxide matrices it has been suggested to absorb as high as 1994 cm^{-1}.[17] Reviewing the data from ref. 39, where values were reported for the isotopomers within an argon matrix, we note that typically, upon isotopic substitution of the terminal carbon atom to ^{13}C, a red-shift of only 4 cm^{-1} is observed. Here, they reported the band positions for the ν_2 stretch of CCO and ^{13}CCO at 1978, and 1974 cm^{-1}; $C^{13}CO$ and $^{13}C^{13}CO$ at 1931 and 1927 cm^{-1}; and for $CC^{18}O$ and $^{13}CC^{18}O$ at 1944 and 1940 cm^{-1}, respectively. Corresponding values taken from ref. 38 for $CC^{18}O$ and $^{13}CC^{18}O$ within an argon matrix were reported as 1934 and 1928 cm^{-1}, respectively. Fig. 1(e) shows this region of the infrared spectrum before and after irradiation. As noted in Table 2, due to the absorptions at 1950 and 1957 cm^{-1} prior to

Table 1 Positions of assigned species identified within the $^{13}CO:C^{18}O$ ice mixture prior to irradiation. Tentative assignments are written in *italics*

Wavenumber/cm^{-1}	Assignment	Characterization
4254	CO $2\nu_1$	Overtone
4157	^{13}CO $2\nu_1$	Overtone
4149	$C^{18}O$ $2\nu_1$	Overtone
2346	CO_2 (ν_3)	Asymmetric stretch
2329	^{18}OCO (ν_3)	Asymmetric stretch
2311	$C^{18}O_2$ (ν_3)	Asymmetric stretch
2280	$^{13}CO_2$ (ν_3)	Asymmetric stretch
2263	$^{18}O^{13}CO$ (ν_3)	Asymmetric stretch
2245	$^{13}C^{18}O_2$ (ν_3)	Asymmetric stretch
2169, 2158	^{13}CO ($\nu_1 + \nu_L$) + $C^{18}O$ ($\nu_1 + \nu_L$)	Lattice mode
2140, 2136	CO (ν_1)	Fundamental
2111	*$C^{17}O$* (ν_1)	Fundamental
2097	*$^{13}C^{18}O$* ($\nu_1 + \nu_L$)	Lattice mode
2090	^{13}CO (ν_1)	Fundamental
2086	$C^{18}O$ (ν_1)	Fundamental
2064	*$^{13}C^{17}O$* (ν_1)	Fundamental
2040	$^{13}C^{18}O$ (ν_1)	Fundamental
636	$^{18}O^{13}CO$ (ν_2)	In-plane/out-of-plane bend

Table 2 Peak position and assignments for the low-molecular weight products detected after the irradiation at 10 K. Tentative assignments have been listed in *italics*

Peak position/cm^{-1}	Assignment	Characterization
4254	CO ($2\nu_1$)	Overtone
4157	^{13}CO ($2\nu_1$)	Overtone
4149	$C^{18}O$ ($2\nu_1$)	Overtone
3714, 3705	CO_2 ($\nu_1 + \nu_3$)	Combination
3680	*^{17}OCO* ($\nu_1 + \nu_3$)	Combination
3668, 3665	^{18}OCO ($\nu_1 + \nu_3$)	Combination
3626	$C^{18}O_2$ ($\nu_1 + \nu_3$), $^{13}CO_2$ ($\nu_1 + \nu_3$)	Combination
3580	$^{18}O^{13}CO$ ($\nu_1 + \nu_3$)	Combination
3561	^{18}OCO ($2\nu_2 + \nu_3$)	Combination
3518, 3515	$C^{18}O_2$ ($2\nu_2 + \nu_3$), $^{13}CO_2$ ($2\nu_2 + \nu_3$)	Combination
3478	$^{18}O^{13}CO$ ($2\nu_2 + \nu_3$)	Combination
2346	CO_2 (ν_3)	Asymmetric stretch
2329	^{18}OCO (ν_3)	Asymmetric stretch
2311	$C^{18}O_2$ (ν_3)	Asymmetric stretch
2280	$^{13}CO_2$ (ν_3)	Asymmetric stretch
2263	$^{18}O^{13}CO$ (ν_3)	Asymmetric stretch
2245	$^{13}C^{18}O_2$ (ν_3)	Asymmetric stretch
2140, 2136	CO (ν_1)	Fundamental
2111	*$C^{17}O$* (ν_1)	Fundamental
2097	*$^{13}C^{18}O$* ($\nu_1 + \nu_L$)	Lattice mode
2090	^{13}CO (ν_1)	Fundamental
2086	$C^{18}O$ (ν_1)	Fundamental
2063	*$^{13}C^{17}O$* (ν_1)	Fundamental
2039	$^{13}C^{18}O$ (ν_1)	Fundamental
1940	$C^{13}CO$ (ν_2)	CO stretch
1937	$^{13}C^{13}CO$ (ν_2)	CO stretch
654	^{18}OCO (ν_2)	In-plane/out-of-plane bend
650	$C^{18}O_2$ (ν_2)	In-plane/out-of-plane bend
640	$^{13}CO_2$ (ν_2)	In-plane/out-of-plane bend
636	$^{18}O^{13}CO$ (ν_2)	In-plane/out-of-plane bend
565, 560, 546, 539, 532, 527, 522	*C_3O_2 isotopomers* (ν_5/ν_6)	CCO bend

irradiation, we were only able to confirm the position of two additional peaks at 1940 and 1937 cm^{-1}. Given the blue-shift observed within a carbon monoxide matrix, we assign these features to the $C^{13}CO$ and $^{13}C^{13}CO$ isotopomers, respectively. Although a deconvolution was attempted to identify other isotopomers, the results of the deconvolution fits were found to be not unique. Note however, that no strong absorptions were identified for the $^{12/13}C^{13}C^{18}O$ isotopomers of this species.

In addition, we expect the formation of isotopomers of species analogous to those previously identified in the irradiation of pure carbon monoxide ices. (ref. 24). These include linear isomers of C_3, C_6, C_nO (n = 3–7), and C_nO_2 (n = 3–5). While the identification of some of these species has been included in Table 2, the remaining unassigned peaks are expected to be from various isotopomers of these species. These peaks were found at: 2226, 2223, 2175, 2172, 2161, 2147w, 2130, 2071, 2010w, 2005w, 2001w, 1981*, 1957*, 1950*, 1928w*, 1811w, 1803w, 490, and 476 cm^{-1} (where an asterisk indicates that these peaks were present prior to irradiation, and 'w' indicates a very weak absorption feature).

3.2 Quadrupole mass spectrometry

Besides the infrared spectra, we also monitored the gas phase. During the irradiation, no electron-stimulated desorption of the ice was found to occur within the detection limits of our spectrometer ($\sim 10^{-15}$ Torr). Therefore, this section focuses on those molecules observed during the heating phase of the irradiated sample. Fig. 2a depicts the results recorded at mass-to-charge (m/z) ratios from $m/z = 28$ to 31 corresponding to the isotopomers of carbon monoxide subliming during the warm-up period. Here, the majority of the ^{13}CO ($m/z = 29$) : $C^{18}O$ ($m/z = 30$) ice sublimates within the range of 24–44 K peaking at around 35 K. The two most abundant peaks from $C^{18}O$ and ^{13}CO are found to overlap during the entire sublimation process. The corresponding signals from CO ($m/z = 28$) and $^{13}C^{18}O$ ($m/z = 31$) are shown also to be very similar; the signal is almost two orders of magnitude weaker than for the other isotopomers. We also searched for signals from O_2 isotopomers ($m/z = 32$ to 36). Here, a trace signal from O_2 ($m/z = 32$) was detected subliming concurrently with the carbon monoxide ices (31–38 K), however, as no signal from the other two isotopomers could be detected this likely originates from impurity within our gas samples. Fig. 2b shows the results from the mass spectrometer for the CO_2 isotopomers ($m/z = 44$ to $m/z = 49$) during the warm-up period. Note that although a small amount of carbon dioxide is lost when the carbon monoxide matrix sublimes, the majority of it remains present on the target until it sublimes over the range of 64–107 K. In pure carbon dioxide ices, the matrix was found to have sublimed completely by 94 K.[28] The detected molecules are consistent with those found spectroscopically, in that the four most abundant isotopomers (^{18}OCO, $C^{18}O_2$, $^{13}CO_2$, and $^{18}O^{13}CO$) give the largest detected signal, whereas a lesser signal is detected for the CO_2 and $^{13}C^{18}O_2$ isotopomers. Note that at this time, a small peak amount of $^{13}C^{18}O$ is also detected between 76–87 K (Fig. 2a), which was presumably trapped within the ice.

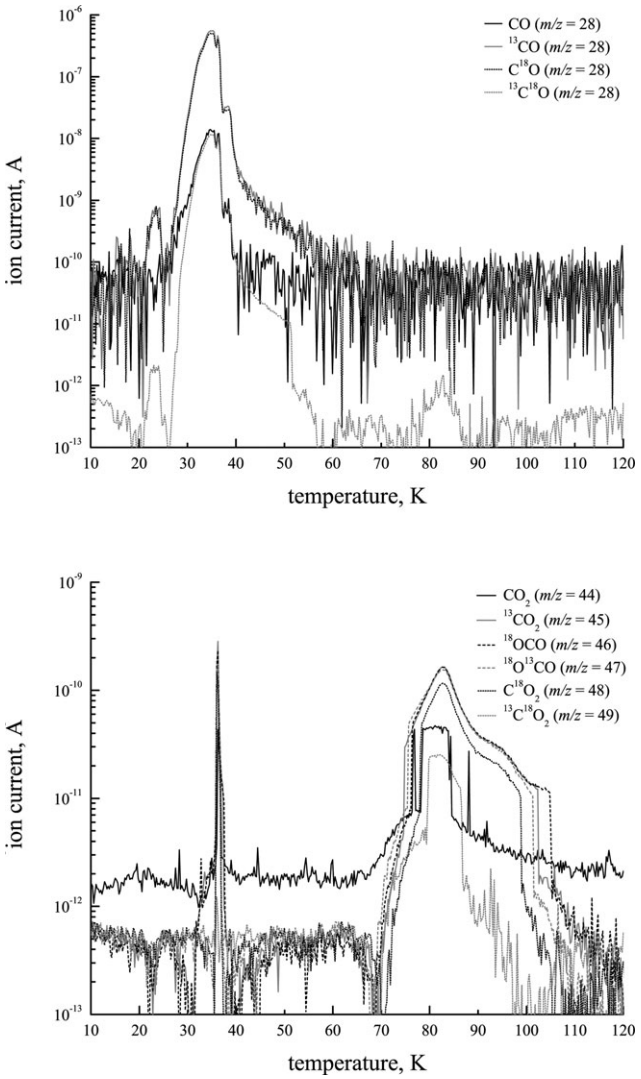

Fig. 2 (a) Ion current recorded by the mass spectrometer for various carbon monoxide isotopomers observed during the warm-up phase; CO ($m/z = 28$; solid black line), ^{13}CO ($m/z = 29$; solid gray line), $C^{18}O$ ($m/z = 30$; dotted black line), and $^{13}C^{18}O$ ($m/z = 31$; dotted gray line). (b) Ion current recorded by the mass spectrometer for various carbon dioxide isotopomers observed during the warm-up phase; CO_2 ($m/z = 44$; solid black line), $O^{13}CO$ ($m/z = 45$; solid gray line), ^{18}OCO ($m/z = 46$; dashed black line), $^{18}O^{13}CO$ ($m/z = 47$; dashed gray line), $C^{18}O_2$ ($m/z = 48$; dotted black line), and $^{13}C^{18}O_2$ ($m/z = 49$; dotted gray line).

4. Discussion

4.1 Kinetic analysis

In order to establish the destruction mechanisms for carbon monoxide and the formation pathways for carbon dioxide, the temporal profiles of the carbon monoxide and carbon dioxide isotopomers were generated by fitting Gaussians to the infrared absorptions to derive the peak areas throughout the hour irradiation period. Column densities were subsequently derived as described in ref. 28, where the error limits reported are 1σ values reported from the deconvolution process. Firstly, considering the destruction of the ^{13}CO and $C^{18}O$ reactant isotopomers of carbon monoxide, we used an exponential decay profile to model its temporal profile which was generated from the overtone bands at 4157 and 4149 cm^{-1}, respectively, using the absorption coefficient of 1.6×10^{-19} cm molecule^{-1}.[29] Thus, the actual temporal profile of the column density of carbon monoxide was fitted using the following decay profiles:

$$[^{13}CO]_t = [^{13}CO]_0 e^{-k_1 t} \quad (1)$$

$$[C^{18}O]_t = [C^{18}O]_0 e^{-k_2 t} \quad (2)$$

Here, $[CO]_t$ is the column density at time t, and $[CO]_0$ is the initial column density of carbon monoxide. The results from the fit for ^{13}CO are depicted in Fig. 3(a), where $[^{13}CO]_0 = 2.07 \pm 0.02 \times 10^{17}$ molecules cm^{-2} and $k_1 = 3.65 \pm 0.54 \times 10^{-5}$ s^{-1}. The values derived for $C^{18}O$ were found to be $[C^{18}O]_0 = 1.84 \pm 0.03 \times 10^{17}$ molecules cm^{-2} and $k_2 = 5.00 \pm 0.78 \times 10^{-5}$ s^{-1} (Fig. 3(b)). The amounts of ^{13}CO and $C^{18}O$ predicted to be destroyed is therefore determined to be $2.5 \pm 0.3 \times 10^{16}$ molecules cm^{-2} and $3.0 \pm 0.3 \times 10^{16}$ molecules cm^{-2}, respectively.

Regarding the formation of the isotopomers of carbon dioxide (Fig. 4), this molecule can be produced either from

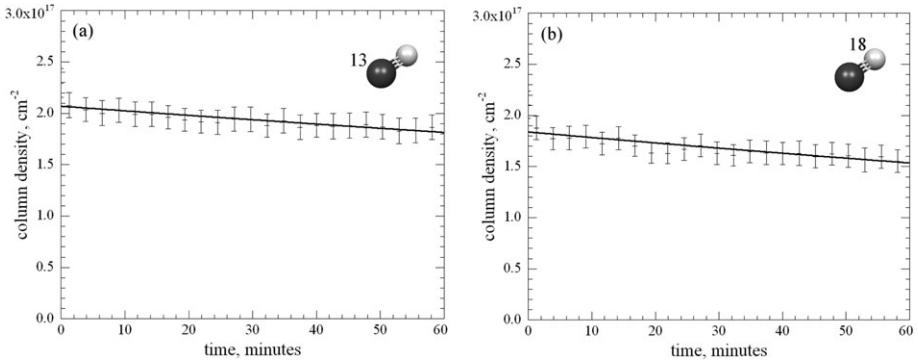

Fig. 3 Temporal evolution of the column densities of two isotopomers of carbon monoxide during the irradiation: (a) ^{13}CO, and (b) $C^{18}O$. Fits are overlaid as discussed in the text.

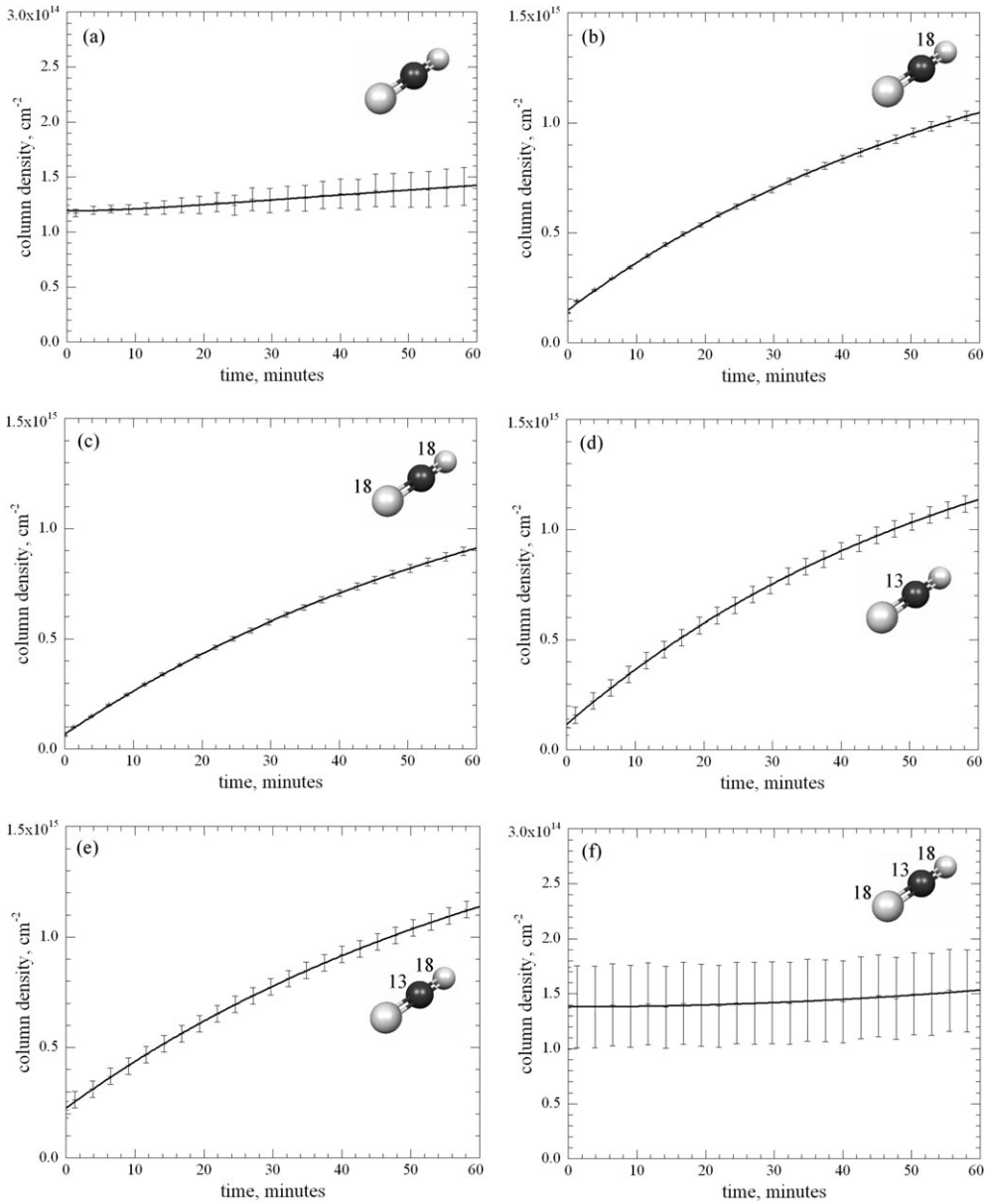

Fig. 4 Temporal evolution of the column densities of the isotopomers of carbon dioxide during the irradiation: (a) CO_2, (b) ^{18}OCO, (c) $C^{18}O_2$, (d) $^{13}CO_2$, (e) $^{18}O^{13}CO$, and (f) $^{13}C^{18}O_2$. Fits are overlaid as discussed in the text.

two carbon monoxide molecules forming carbon dioxide plus a carbon atom[40] and/or from the recombination of an oxygen atom with carbon monoxide; the oxygen atom can be formed by unimolecular decomposition of the carbon monoxide molecule upon interaction with the energetic electrons.[17] For each carbon dioxide isotopomer, the temporal profile was fit using (pseudo) first order kinetics. The ν_3 asymmetric stretch was employed to derive the column densities, combined with the absorption coefficient of 8.0×10^{-17} cm molecule^{-1}.[41] The results show that the isotopomers ^{18}OCO, C^{18}O$_2$, ^{13}CO$_2$, and ^{18}O^{13}CO could be fit using pseudo first order kinetics with the following equations:

$$[^{18}\mathrm{OCO}]_t = a(1 - e^{-k_3 t}) \quad (3)$$

$$[\mathrm{C}^{18}\mathrm{O}_2]_t = b(1 - e^{-k_4 t}) \quad (4)$$

$$[^{13}\mathrm{CO}_2]_t = c(1 - e^{-k_5 t}) \quad (5)$$

$$[^{18}\mathrm{O}^{13}\mathrm{CO}]_t = d(1 - e^{-k_6 t}) \quad (6)$$

Here, the results for ^{18}OCO were found to be $a = 1.46 \pm 0.02 \times 10^{15}$ molecules cm^{-2}, and $k_3 = 2.64 \pm 0.07 \times 10^{-4}$ s^{-1} (Fig. 4(b)). For C^{18}O$_2$, the data suggest that $b = 1.46 \pm 0.13 \times 10^{15}$ molecules cm^{-2}, k_4 $2.39 \pm 0.04 \times 10^{-4}$ s^{-1} (Fig. 4(c)). Considering ^{13}CO$_2$, we derived $c = 1.60 \pm 0.02 \times 10^{15}$ molecules cm^{-2} and $k_5 = 2.82 \pm 0.05 \times 10^{-4}$ s^{-1} (Fig. 4(d)). Finally, for ^{18}O^{13}CO, the results were $d = 1.58 \pm 0.02 \times 10^{15}$ molecules cm^{-2}, $k_6 = 2.39 \pm 0.05 \times 10^{-4}$ s^{-1} (Fig. 4(e)). For the other two isotopomers of carbon dioxide, we were unable to fit the results using a (pseudo) first order kinetic scheme. After consideration of the proposed mechanisms (next section) these profiles were fit using a two-step sequential mechanism[42] (shown in Fig. 4(a,f)), however, we were unable to find unique fits.

4.2 Reaction mechanisms

The proposed reaction mechanisms have to account for the following experimental findings (F1–F5) as summarized from the prior discussion:

F1: The destruction profiles of ^{13}C^{16}O and ^{12}C^{18}O could be fit with (pseudo) first order kinetics; the inherent rate constants of $k_1 = 3.65 \pm 0.54 \times 10^{-5}$ s^{-1} and $k_2 = 5.00 \pm 0.78 \times 10^{-5}$ s^{-1} are of the same magnitude.

F2: During the irradiation, two new isotopomers of carbon monoxide were formed: ^{12}C^{16}O and ^{13}C^{18}O.

F3: During the irradiation, four isotopomers of carbon dioxide (^{18}OCO, C^{18}O$_2$, ^{13}CO$_2$, and ^{18}O^{13}CO) dominate the product spectrum in equal amounts. The temporal profiles could be fit using pseudo first order kinetics with rate constants of $k_3 = 2.64 \pm 0.07 \times 10^{-4}$ s^{-1}, k_4 $2.39 \pm 0.04 \times 10^{-4}$ s^{-1}, $k_5 = 2.82 \pm 0.05 \times 10^{-4}$ s^{-1}, and $k_6 = 2.39 \pm 0.05 \times 10^{-4}$ s^{-1}. Within the error limits, these rate constants are identical.

F4: To a minor amount, the formation of two additional isotopomers of carbon dioxide was monitored (^{13}C^{18}O$_2$, ^{12}C^{16}O$_2$). The temporal profiles could be only fit with two-step mechanisms, but not with a (pseudo) first order kinetics.

F5: No appreciable amounts of isotopomers of molecular oxygen, or ozone were detectable throughout the experiments.

A literature review reveals that in principle two reaction mechanisms have been proposed. As suggested by Gerakines *et al.*,[17] energetic ions and electrons are capable of dissociating the carbon monoxide molecule as depicted in reaction (7). The oxygen atoms released could react with carbon monoxide to form a carbon dioxide molecule (eqn (8). Note that while no barrier exists for the reaction with excited oxygen atoms, in the case of ground state oxygen atoms, an initial addition barrier of 0.26 eV has to be overcome;[43] in addition, intersystem crossing from the triplet to the singlet surface has to be involved, which may take place before or after carbon dioxide is formed; these spin-forbidden processes may be mediated by the surrounding ice medium. Here, the overall reaction sequence is defined as M1 (mechanism 1).

$$\mathrm{CO}(\mathrm{X}^1\Sigma^+) \rightarrow \mathrm{C}(^3\mathrm{P}/^1\mathrm{D}) + \mathrm{O}(^3\mathrm{P}/^1\mathrm{D}) \quad (7)$$

$$\mathrm{O}(^3\mathrm{P}/^1\mathrm{D}) + \mathrm{CO}(\mathrm{X}^1\Sigma^+) \rightarrow \mathrm{CO}_2(\mathrm{X}^1\Sigma_g^+) \quad (8)$$

Photodissociation experiments of pure carbon monoxide ices suggest an alternative pathway, hereafter referred to as M2 (mechanism 2). Note that a recent experimentally determined value for this dissociation energy is given as 11.09 eV;[44] this requires photons of wavelength below 112 nm for photodissociation to occur.[40] However, a typical broadband hydrogen discharge lamp has the most intense band at 121 nm (10.2 eV; Lyman-α); this source has only considerable flux for photons within the range 7.3–10.5 eV.[45] It is obvious that a different mechanism than (7) and (8) must be responsible for initiating the reactions. It has been considered that a photon first excites the carbon monoxide into an excited state; this excited molecule can then react with a neighboring carbon monoxide molecule to produce carbon dioxide and ground state carbon atoms:[24]

$$\mathrm{CO}(\mathrm{X}^1\Sigma^+) \rightarrow \mathrm{CO}^* \quad (9)$$

$$\mathrm{CO}^* + \mathrm{CO}(\mathrm{X}^1\Sigma^+) \rightarrow \mathrm{CO}_2(\mathrm{X}^1\Sigma_g^+) + \mathrm{C}(^3\mathrm{P}) \quad (10)$$

The overall reaction from two ground state carbon monoxide molecules is endoergic by only 5.64 eV, and there is experimental evidence supporting the fact that the excited state involved is the metastable a$^3\Pi$ state,[46] which lies 6.0 eV above the ground state.[47] This production mechanism seems to support the species observed in experiments on the irradiation of carbon monoxide by photolysis,[16,17] in particular since matrix isolated carbon monoxide failed to produce carbon dioxide when exposed to irradiation within a nitrogen matrix.[18] This mechanism was also identified as the sole destruction pathway for carbon monoxide in pure carbon monoxide to account for the observed production of newly formed species like oxygen-terminated carbon clusters, where pure ices were subjected to energetic electrons.[24] This is supported by the fact that the inelastic energy loss processes occurring during the processing of carbon monoxide by energetic electrons have been shown to effectively excite carbon monoxide into the a$^3\Pi$ state.[47]

Based on the experimental findings F1 to F5, we are discussing now if mechanism M1 or M2 (or both) can account for our experimental data. The predominant finding is the fact that four carbon dioxide isotopomers ^{18}OCO, C^{18}O$_2$, ^{13}CO$_2$,

and $^{18}O^{13}CO$ are produced in equal amounts and identical rate constants (F4). This strongly indicates that the underlying reaction pathways to synthesize these species are identical. The $^{13}C^{16}O$ and $^{12}C^{18}O$ reactants were homogeneously mixed in the gas phase; the resulting ice mixture is also expected to be homogeneous. In this case, the electron beam could result in the formation of electronically excited $^{13}C^{16}O^*$ and $^{12}C^{18}O^*$. Both of these species can react with a neighboring $^{13}C^{16}O$ *and* $^{12}C^{18}O$ molecule resulting in the formation of distinct molecules *via* eqn (11)–(14):

$$^{13}C^{16}O^* + {}^{13}C^{16}O(X^1\Sigma^+) \rightarrow {}^{13}C^{16}O_2(X^1\Sigma_g^+) + {}^{13}C(^3P) \quad (11)$$

$$^{13}C^{16}O^* + {}^{12}C^{18}O(X^1\Sigma^+) \rightarrow {}^{18}O^{12}C^{16}O(X^1\Sigma^+) + {}^{13}C(^3P) \quad (12a)$$

$$\rightarrow {}^{18}O^{13}C^{16}O(X^1\Sigma^+) + {}^{12}C(^3P) \quad (12b)$$

$$^{12}C^{18}O^* + {}^{13}C^{16}O(X^1\Sigma^+) \rightarrow {}^{18}O^{12}C^{16}O(X^1\Sigma^+) + {}^{13}C(^3P) \quad (13a)$$

$$\rightarrow {}^{18}O^{13}C^{16}O(X^1\Sigma^+) + {}^{12}C(^3P) \quad (13b)$$

$$^{12}C^{18}O^* + {}^{12}C^{18}O(X^1\Sigma^+) \rightarrow {}^{12}C^{18}O_2(X^1\Sigma_g^+) + {}^{12}C(^3P) \quad (14)$$

Formally, the formation of the carbon dioxide species *via* mechanism M2 can be fit with (pseudo) first order kinetics; the identical rate constants for these processes as compiled in F3 suggest no isotopic enrichment within the error limits. It should be stressed that the sequential mechanism M1 is unlikely. Most important, eqn (7) suggests the existence of *free* oxygen atoms. Even at 10 K, the initially generated oxygen atoms are suprathermal and hence can diffuse. This should not only result in reaction (8), *i.e.* a reaction of the free oxygen atom with carbon monoxide, but also in the formation of *molecular oxygen* in carbon monoxide ices.[28] However, as F5 states, during the electron exposure of carbon monoxide ices, no strong evidence for the production of molecular oxygen was observed through mass spectrometry. In addition, it is expected that *free* oxygen atoms in the presence of molecular oxygen would further react to produce *ozone*,[48] also not observed through infrared spectroscopy. This argument suggests that reaction mechanism M2 presents the most likely dominating reaction pathway to form carbon dioxide, at least in ices of pure carbon monoxide and isotopic mixtures of carbon monoxide.

It is interesting to comment briefly on the observation of minor amounts of $^{12}C^{16}O$ and $^{13}C^{18}O$ (F2) and of $^{13}C^{18}O_2$ and $^{12}C^{16}O_2$ (F4). The dominating reaction mechanism M2 cannot account for the synthesis of these species. The kinetic fits are not sensitive to destruction channels of the carbon dioxide molecules, if these pathways account for a few per cent of the loss processes. Recall that the experimental error bars of the integrated band profiles are at the 10% level. Therefore, an incorporation of a minor destruction of the carbon dioxide isotopomers ^{18}OCO, $C^{18}O_2$, $^{13}CO_2$, and $^{18}O^{13}CO$ could result also into small amounts of $^{12}C^{16}O$ (from ^{18}OCO) and $^{13}C^{18}O$ (from $^{18}O^{13}CO$). This is consistent with results on electron irradiation of pure carbon dioxide ices where the direct formation of carbon monoxide was observed.[28] A reaction of electronically excited $^{12}C^{16}O^*$ and $^{13}C^{18}O^*$ with $^{12}C^{16}O$ and $^{13}C^{18}O$ can form *via* mechanism M2 $^{12}C^{16}O_2$ and $^{13}C^{18}O_2$, respectively. This would require a multi step mechanism and verified by the kinetic fits of the $^{12}C^{16}O_2$ and $^{13}C^{18}O_2$ profiles. However, it should be noted that reaction mechanism M1 cannot be entirely ruled out as a pathway to produce minor amounts of $^{12}C^{16}O$ and $^{13}C^{18}O$ (F2) *via* the recombination of atomic C and O atoms.

5. Conclusion

This paper focused on the processing of binary ice mixtures of two carbon monoxide isotopomers, $^{13}C^{16}O$ and $^{12}C^{18}O$, by energetic electrons at 10 K. The most likely reaction pathways leading to the formation of four carbon dioxide isotopomers ^{18}OCO, $C^{18}O_2$, $^{13}CO_2$, and $^{18}O^{13}CO$ was suggested to involve an initial electronic excitation of the $^{13}C^{16}O$ and $^{12}C^{18}O$ reactants by the energetic electrons followed by a reaction of the electronically excited molecules with ground state, neighboring $^{13}C^{16}O$ and $^{12}C^{18}O$ molecules. The resulting temporal profiles could be fit with (pseudo) first order kinetics thus underlining the proposed reaction mechanism. Alternative reaction processes involving the unimolecular decomposition of carbon monoxide into carbon and oxygen atoms are unlikely since in irradiated pure and isotopic mixtures of carbon monoxide ices, within the detection limits of our experiment, no appreciable molecular oxygen—a reaction product resulting from recombination of two oxygen atoms—was observed.

References

1 J. S. Young and N. Z. Scoville, *Annu. Rev. Astron. Astrophys.*, 1991, **29**, 581.
2 E. F. van Dishoeck and J. H. Black, *Astrophys. J.*, 1988, **334**, 771.
3 Y. Aikawa, N. Ohashi, S.-I. Inutsuka and E. Herbst, *Astrophys. J.*, 2001, **522**, 639.
4 Y. Aikawa, V. Wakelem, R. T. Garrod and E. Herbst, *Astrophys. J.*, 2008, **674**, 984.
5 E. L. Gibb, D. C. B. Whittet, A. C. A. Boogert and A. G. G. M. Tielens, *Astrophys. J., Suppl. Ser.*, 2004, **151**, 35.
6 D. C. B. Whittet, S. S. Shenoy, E. A. Bergin, J. E. Chiar, P. A. Gerakines, E. L. Gibb, G. J. Melnick and D. A. Neufeld, *Astrophys. J.*, 2007, **655**, 332.
7 S. S. Prasad and S. P. Tarafdar, *Astrophys. J.*, 1983, **267**, 603.
8 G. Strazzulla and R. E. Johnson, *Comets in the Post-Halley Era*, Kluwer, Dordrecht, 1991.
9 R. I. Kaiser, *Chem. Rev.*, 2002, **102**, 1309.
10 J. W. T. Spinks and R. J. Woods, *An Introduction to Radiation Chemistry*, Wiley, New York, 1990.
11 R. I. Kaiser and K. Roessler, *Astrophys. J.*, 1997, **475**, 144.
12 R. I. Kaiser, G. Eich, A. Gabrysch and K. Roessler, *Astrophys. J.*, 1997, **484**, 487.
13 R. E. Johnson, *Energetic Charged-Particle Interactions with Atmospheres and Surfaces*, Springer-Verlag, Berlin, 1990.
14 C. J. Bennett, C. S. Jamieson, Y. Osamura and R. I. Kaiser, *Astrophys. J.*, 2005, **624**, 1097.
15 E. Dartois, K. Demyk, M. Gerin and L. d'Hendecourt, *ESA-SP*, Villafranca del Castillo, Spain, 2000.
16 P. A. Gerakines, W. A. Schutte and P. Ehrenfreund, *Astron. Astrophys.*, 1996, **312**, 289.
17 P. A. Gerakines and M. H. Moore, *Icarus*, 2001, **154**, 372.
18 H. Cottin, M. H. Moore and Y. Bénilan, *Astrophys. J.*, 2003, **590**, 874.

19 M. J. Loeffler, G. A. Baratta, M. E. Palumbo, G. Strazzulla and R. A. Baragiola, *Astron. Astrophys.*, 2005, **435**, 587.
20 T. Baird, *Carbon*, 1972, **10**, 723.
21 R. A. Haring, R. Pedrys, D. J. Oostra, A. Haring and A. E. De Vries, *Nucl. Instrum. Methods Phys. Res.*, 1984, **5**, 476.
22 D. B. Chrisey, J. W. Boring, J. A. Phipps, R. E. Johnson and W. L. Brown, *Nucl. Instrum. Methods Phys. Res.*, 1986, **13**, 360.
23 A. Trottier and R. L. Brooks, *Astrophys. J.*, 2004, **612**, 1214.
24 C. S. Jamieson, A. M. Mebel and R. I. Kaiser, *Astrophys. J., Suppl. Ser.*, 2006, **163**, 184.
25 M. H. Moore, R. Khanna and B. Donn, *J. Geophys. Res., [Atmos.]*, 1991, **96**, 17541.
26 N. Watanabe and A. Kouchi, *Astrophys. J.*, 2002, **567**, 651.
27 D. P. Ruffle and E. Herbst, *Mon. Not. R. Astron. Soc.*, 2001, **312**, 1054.
28 C. J. Bennett, C. Jamieson, A. M. Mebel and R. I. Kaiser, *Phys. Chem. Chem. Phys.*, 2004, **6**, 735.
29 P. A. Gerakines, J. J. Bray, A. Davis and C. R. Richey, *Astrophys. J.*, 2005, **620**, 1140.
30 G. J. Jiang, W. B. Person and K. G. Brown, *J. Chem. Phys.*, 1975, **62**, 1201.
31 G. E. Ewing and G. C. Pimentel, *J. Chem. Phys.*, 1961, **35**, 925.
32 S. A. Sandford, L. J. Allamandola, A. G. G. M. Tielens and G. J. Valero, *Astrophys. J.*, 1988, **329**, 498.
33 F. W. Froben, I. Rabin, M. Ritz and W. Schulze, *Z. Phys. D: At., Mol. Clusters*, 1996, **38**, 335.
34 W. B. J. M. Jannsen, J. Michiels and A. van der Avoird, *J. Chem. Phys.*, 1991, **94**, 8402.
35 C. V. Berney and D. F. Eggers Jr, *J. Chem. Phys.*, 1964, **40**, 990.
36 S. A. Sandford and L. J. Allamandola, *Astrophys. J.*, 1990, **355**, 357.
37 J.-L. Teffo, L. Daumont, C. Claveau, A. Valentin, S. A. Tashkun and V. I. Pevalov, *J. Mol. Spectrosc.*, 2002, **213**, 145.
38 R. L. DeKock and W. Weltner Jr, *J. Am. Chem. Soc.*, 1971, **93**, 7106.
39 M. E. Jacox, D. E. Milligan, N. G. Moll and W. E. Thompson, *J. Chem. Phys.*, 1965, **43**, 3734.
40 H. Okabe, *Photochemistry of Small Molecules*, Wiley, New York, 1978.
41 P. A. Gerakines, W. A. Schutte, J. M. Greenberg and E. F. van Dishoeck, *Astron. Astrophys.*, 1995, **296**, 810.
42 J. I. Steinfeld, J. S. Francisco and W. L. Hase, *Chemical Kinetics and Dynamics*, Prentice Hall, Upper Saddle River, 1999.
43 D. Talbi, G. S. G. S. Chandler and A. L. Rohl, *Chem. Phys.*, 2006, **320**, 214.
44 B. L. G. Bakker and D. H. Parker, *Chem. Phys. Lett.*, 2000, **330**, 293.
45 G. M. Muñoz Caro and W. A. Schutte, *Astron. Astrophys.*, 2003, **412**, 213.
46 J.-P. Martin, M.-Y. Perrin and P. I. Porshnev, *Chem. Phys. Lett.*, 2000, **332**, 283.
47 P. W. Zetner, I. Kanik and S. Trajmar, *J. Phys. B*, 1998, **31**, 2395–2413.
48 C. J. Bennett and R. I. Kaiser, *Astrophys. J.*, 2005, **635**, 1362.

